MR DAMPER MONITORING FOR STRUCTURAL APPLICATIONS: EXPERIMENTAL STUDY AND COMPARISON WITH NONLINEAR CONTROL

Sk. Faruque Ali[1], Ananth Ramaswamy[2]
[1]Newton Fellow, School of Engineering, Swansea University, Swansea, UK, SA2 8PP
[2] Department of Civil Engineering, I.I.Sc, Bangalore 560012
E-mail of corresponding author: ananth@civil.iisc.ernet.in

ABSTRACT

The increase in bearing displacements of base isolated buildings due to near-field earthquakes, with long-period pulse type of ground motion, is an important problem. This study investigates the ability of an adaptive seismic isolation system to protect structures subjected to disparate ground motions. An experimental study of a hybrid base-isolated, three-story steel frame building is presented. The isolation system incorporates sliding bearings combined with a magneto-rheological (MR) fluid damper. The damping capacity of the MR damper is modulated in real time with an optimal fuzzy logic control (FLC) algorithm developed for the sole purpose. Shake table tests are conducted to evaluate the effectiveness of the MR damper in reducing the response of the isolated test structure when subjected to both near-field and far-field earthquake excitations. Analytical models of the isolation system components and the test structure are developed and calibrated through experimental system identification tests. Results from tests are used to validate the numerical simulations.

INTRODUCTION

The destructions caused by seismic events over centuries across the world have clearly demonstrated the importance and the need for mitigating the effect of such natural hazards on structures. Base isolation, isolating the structure from incoming seismic waves at its base, is an old and successful technique to protect structures and their contents. The idea of augmenting damping with isolation to dissipate energy under near field seismic motions has been identified as one promising approach in this direction [1]. The possible ways are to use high damping rubber bearings, lead rubber bearings, friction pendulum, etc., or to add damping devices along with rubber bearings [2]. The damping device could be a passive [3, 4], active (e.g., active mass damper) or a semi-active (e.g., MR damper) device. Due to strong nonlinearity, vibration reduction using lead rubber bearings, friction pendulum, sliding bearing, high damping rubber bearing are not optimal over a wide range of seismic excitations [5]. Supplemental passive dampers certainly reduce the base displacements, but they may increase the inter-story drifts and accelerations in the superstructure [6].

A number of researchers have studied adaptive base-isolation systems for seismic protection of buildings using semi-active control devices which require a relatively small amount of power for operation. The forces that develop in such devices are induced by the motion of the structure to which they are attached. Very few experimental studies that employ MR dampers as a supplemental damping device have been reported in the literature compared to numerical studies [5, 7, 8, 9, 10, 11, 12, 13, and 14]. An H2/LQG clipped optimal controller has been reported in [12] for a small-scale rubber bearing system that is augmented with an MR damper. A modified clipped optimal strategy has been applied by [15]. Sliding mode control of sliding-isolated buildings using variable orifice dampers has been studied experimentally by [11]. While in [9,10] the suitability of Lyapunov based on-off strategy for MR damper control of a laboratory scaled base isolated bridge and base isolated two-storey building have been verified.

Various intelligent control methods such as, neural controllers [16, 17] and non-adaptive [18] and adaptive fuzzy controllers [Ali and Ramaswamy 2008] have been attempted with the damper monitoring voltage (or current) directly set based on system feedback. In [19], a comparison of adaptive, non-adaptive and Lyapunov based clipped optimal strategy for a nonlinear base isolated benchmark building has been provided. Very few experimental studies with intelligent controller are reported (e.g., [13, 17, and 19]). These studies have shown a substantial decrease in the acceleration response with only a modest increase in the displacement response.

This paper concentrates on an experimental and numerical study of the seismic response of a three storey steel building frame with an adaptive hybrid seismic isolation system. The isolation system consists of sliding bearings combined with MR dampers. Genetic algorithm based optimal fuzzy logic control approach is used Optimal Fuzzy Logic based Smart Isolation for Buildings to monitor the voltage on the MR damper. This paper explores the efficiency of an optimal fuzzy logic controller developed and reported in [18]. The next section provides details of the experimental set-up followed by a discussion on the mathematical modeling. Details of the control strategy considered and optimization of FLC parameters are then reported. Finally the comparison of experimental results with the corresponding numerical simulations is discussed.

DETAILS OF EXPERIMENTAL PROGRAM

The schematic diagram of the experimental test set-up for hybrid base isolated base-isolated building control using optimal FLC is shown in Fig. 1. The hybrid isolation is achieved using four sliding bearing at the four column bases of the building and an MR damper connected at the base (Fig. 1). The stiffness of the bearing at the base is augmented using four linear springs placed co-axially with the sliding bearings. Figs. 1 and 2 show the position of the linear varying displacement transformers (LVDT) and the accelerometers. Acceleration responses and inter-storey drifts are measured on all floors. In addition, acceleration and relative displacement (w.r.t. shake table) at the base isolator and acceleration and absolute displacement of the shake table are measured.

Data acquisition is carried out using Dewetron acquisition system at a sampling rate of 1 kHz. For real time control implementation dSPACE® [20] real-time controller, which has an on-board digital signal processor (DSP) is used. Thus the processing speed depended only on the DSP, which was designed specifically for real-time tasks. The optimal FLC is encoded in MATLAB® Simulink® [21] using real time workshop (RTW) interface and dSPACE® hardware and software [20]. The isolator acceleration at the damper location and pseudo velocity (obtained by integrating acceleration data in real time) are used as feedback to the RTW to obtain the voltage required by the MR damper. Fig. 3 shows the Simulink block diagram of the controller implementation.

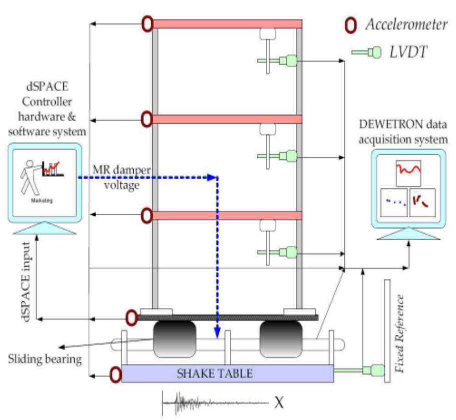

Figure 1: Schematic Diagram of the Experimental Set-up

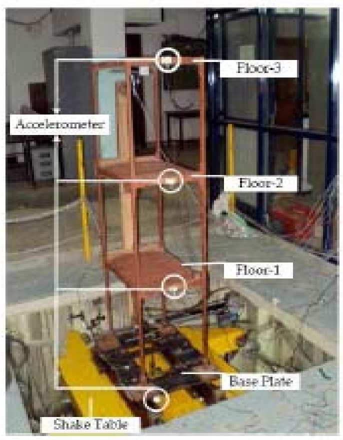

Figure: 2 Experimental Set-ups

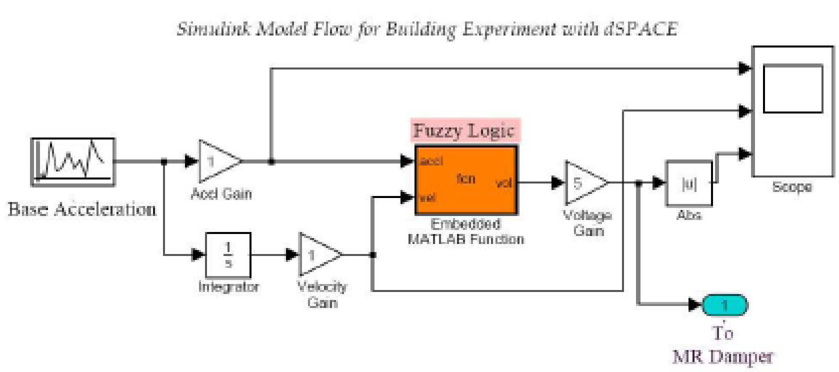

Figure 3: Simulink Diagram of the FLC Implementation

MATHEMATICAL MODELING AND SYSTEM IDENTIFICATION

Impulse hammer tests (IHT) are conducted to determine the fixed base building parameters, while sinusoidal base excitation is used to determine the damping characteristics of the sliding bearings. The stiffness at the base provided by the linear springs is determined experimentally using a servo hydraulic closed loop universal test rig. Simple Bouc-Wen model is used to model MR damper hysteretic characteristic and the procedure has been reported in [22].

A RD-1005-3 MR damper [24], manufactured by Lord® Corporation is used for the experiment study. The damper is 208mm long in its extended position, and 155mmin fully compressed position. The damper can provide a stroke of ±25mm. The input voltage can be varied to a maximum of 2.5 V (continuous supply) and 5 V (intermittent supply). MR damper is tested using a servo hydraulic Universal Testing Machine. Details of the MR damper tests and modeling are reported in [22, 23]. In this paper, the widely used simple Bouc-Wen model [25] is explored to characterize the MR damper implemented in the experimental study. The Bouc-Wen model parameters are obtained from nonlinear least square based model fit of the experimental data. For the present study on seismic vibration mitigation application of the MR damper, the damper parameters used are given in [22]. Fig. 4 shows the match between experimental and analytical model at 10mm amplitude and at a frequency of 0.25Hz, with the current varied between zero and one ampere.

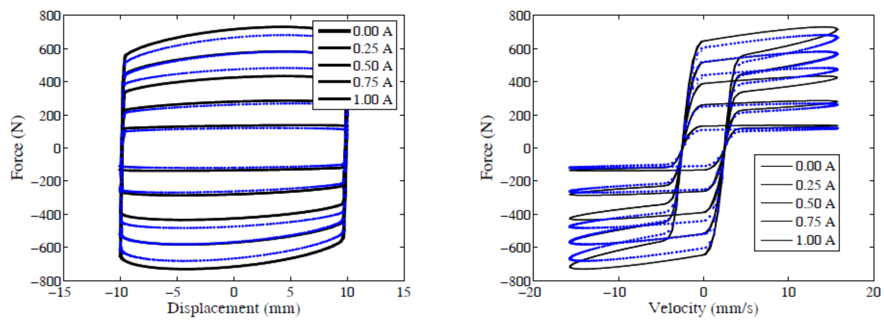

(a) Force displacement loop (b) Force velocity loop

Figure 4: MR damper experimental and analytical hysteretic curves (10 mm amplitude and 0.25 Hz frequency)

The mass of the base is measured to be 38kg. The stiffness of the linear springs attached coaxially with the sliding isolator was measured using servo-hydraulic testing machine. The stiffness of each of the springs is found to be 2.162kN/m. A nonlinear frictional damping ($fb = \mu w z_w$) is considered for the isolator, here μ is the coefficient of friction at the bearing and w is the normal load at the bearing. zw is the Wen's hysteretic parameter used to model friction [9, 10]. The coefficient of friction at the bearing [9, 11] is given by eq. (1),

$$\mu = \mu_{\max} - (\mu_{\max} - \mu_{\min}) e^{-\lambda |\dot{x}_b|} \tag{1}$$

where μ ranges from μ_{max} at large velocities of sliding to μ_{min} at very low velocities. λ is a constant having units of time per unit length and $\dot{x}_b$ is the velocity across the isolator. The values to μ_{max} and μ_{min} are determined through experiments tests. The Wen's hysteretic variable (z_w) is given by [9] as eq.(2),

$$Y \dot{z}_w + \gamma_w |\dot{x}_b| z_w + \beta_w \dot{x}_b z_w^2 - A_w \dot{x}_b = 0 \tag{2}$$

where the constants Y , A_w, γ_w, and β_w are the shape parameters of the hysteretic loop which are calibrated using the experimental data. Tests with sinusoid input excitations at the base are carried out with varied frequencies ranging from 1Hz to 3Hz and amplitudes ranging from 2mm to 10mm, to determine frictional damping at the sliding isolator. Particle swarm optimization algorithm is used to optimize the variables, μ_{max}, μ_{min}, Y and ¸. The values for

A_w, γ_w and β_w are considered as 1, 0.9 and 0.1, respectively [9, 11]. The optimal values for the variables are obtained as μ_{max} = 1.1303, μ_{min} = 0.2853, Y = 0.2526 and λ = 0.6191.

A RD-1005-3 MR damper [24], manufactured by Lord® Corporation is used for the experimental study. The damper is 208mm long in its extended position, and 155mmin fully compressed position. The damper can provide a stroke of ±25mm. The input voltage can be varied to a maximum of 2.5 V (continuous supply) and 5 V (intermittent supply). MR damper is tested using a servo hydraulic Universal Testing Machine. Details of the MR damper tests and modeling are reported in [22, 23]. In this paper, the widely used simple Bouc-Wen model [25] is explored to characterize the MR damper implemented in the experimental study. The Bouc-Wen model parameters are obtained from nonlinear least square based model fit of the experimental data. For the present study on seismic vibration mitigation application of the MR damper, Fig. 5 shows the match between experimental and analytical model at 10mm amplitude and at a frequency of 0.25Hz, with the current varied between zero and one ampere.

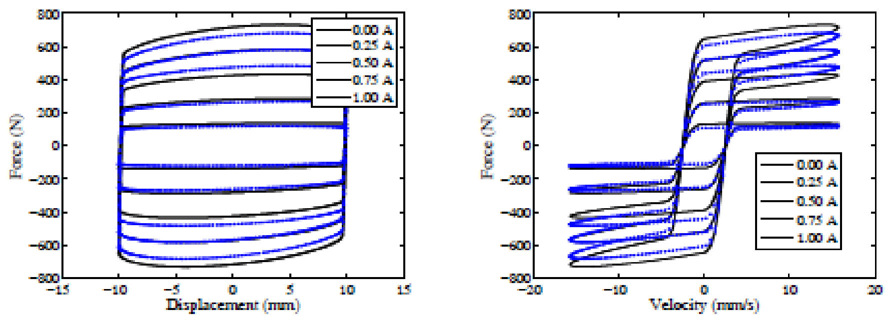

(a) Force displacement loop (b) Force velocity loop

Figure 5 MR damper experimental and analytical hysteretic curves (10 mm amplitude and 0.25 Hz frequency)

CONTROL ALGORITHM FOR MR DAMPER MONITORING

The experimental study is carried out considering both near-fault and far-fault seismic excitations. Tests with (a) fixed base condition (building without isolator and MR damper), (b) building with only base isolation, and (c) Hybrid isolation i.e., simple base isolation supplemented with a single MR damper. The MR damper is operated in two passive conditions with 0 V and 2.5 V. A manually designed FLC (SFLC) and a genetic algorithm optimized FLC (GAFLC) are employed to provide variable voltage input to the MR damper.

The performances of conventional controllers (LQG, H2 etc.) depend on the accuracy in modeling of the system dynamics and are effective in control of linear structural behavior. As an alternative to conventional control theory, FLC allows the resolution of imprecise or uncertain information. It maps the nonlinear input-output relation effectively and also handles the hysteretic behavior of structures under earthquake loads with ease. Furthermore, FLC output [v(t)], used to monitor the voltage requirement of the MR damper, can take any value between [0, 1] and therefore covers full voltage range available for the damper [18]. In the process, the voltage switch is gradual and does not jump between zero and maximum values as in Lyapunov or LQG clipped optimal control cases. This paper presents experimental studies on two FLCs, (i) FLC with manually designed rule base (SFLC) and (ii) GA optimized FLC rule base (GAFLC). The FLC parameters optimized in GAFLC are the input-output membership functions (MFs), scaling gains and the fuzzy rule base [23]. The FLCs (SFLC and GAFLC) have two input variables namely, acceleration and velocity, at the damper location and provide MR damper voltage as an output. The input/output variables are normalized over the UOD (universe of discourse) of [−1, 1]. The input variables range their respective UOD using five equally spaced 'gbell' shaped MFs (NL = Negative Large, NS = Negative Small, ZE = Zero, PS=Positive Small, PL = Positive Large). Seven equally spaced 'gbell' shaped MFs are used to define the output voltage (v(t) 2 [0, 1]), which is then passed to MR damper (PO=Positive; NE=Negative MFs are extra MFs). The extreme MFs for input variables are kept unbounded in the respective positive (s-shaped) and negative (z-shaped) UOD. This is done to consider the values of input that are outside the range of UOD. It is to be noted that the output contains negative values, which is done to keep symmetry about the zero in UOD.

In this paper micro-GA [26] is used to automatically generate the rule base, MF parameters and scaling gains in order to optimize the FLC response. For the GA used in this study, each chromosome represented a complete FLC as defined by [21] fuzzy inference files (FIS). The rule base is modified using a geometric approach keeping the symmetry in the rule base structure. The geometric approach requires fewer optimization variables and thereby reduces the chromosome length. This reduces the computational overhead of the optimization scheme. The geometric approach is shown in Fig. 6. The consequent space (space spanned by the output MFs) is over-layed upon the 'premise coordinate system' (space spanned by the input MFs) and is in effect partitioned into seven non-overlapping small regions. Each region represents a consequent fuzzy set. The design of the optimal rule base is achieved using the consequent line as shown in Fig. 6. The line is made pivotal on premise zero-zero position (i.e., both inputs being zero) and it is free to rotate over the consequent space. Each specific position of the consequent line provided a new rule base. Therefore the slope of the consequent line (CA) is encoded as an optimization variable. It is to be noted that the rule base remains symmetrical whatever be the position (orientation) of the consequent line. The rule base is then extracted by determining the consequent region, in which, each premise combination point lies. Next a consequent- region spacing (CS) is encoded to define the distance between consequent points along the consequent line. These two optimization variables (CA and CS) provide an optimal rule selection. The MF properties altered by the GA are MF shape, MF center shift and MF slope at 0.5 membership grade. Details on micro-GA encoding of optimal FLC has been reported in [22, 23]. For the experimental study an off-line trained FLC is adopted. The off-line training is carried out by providing an initial base displacement of 0.025m and then allowing the hybrid system to come to rest. The FLC that minimizes the following cost function is adopted for the experimental study is as shown in eq.(3).

$$J_{ga} = \| \frac{x_b}{x_{bunc}} \| + \| \frac{\ddot{x}_b}{\ddot{x}_{bunc}} \| \tag{3}$$

The above cost function considers minimization (L2 norm) of the ratio of base displacement (x_b) with controller and base displacement (x_{bunc}) with-out controller and at the same time minimizing the corresponding ratio of acceleration norms. Fig. 7 shows the rule base surface obtained from the optimization process.

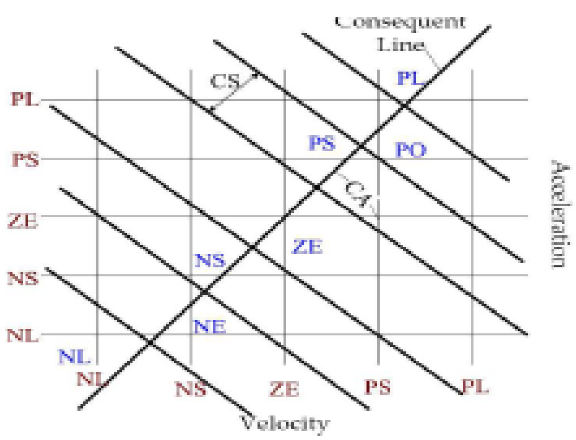

Figure 6: Adaptive rule base design

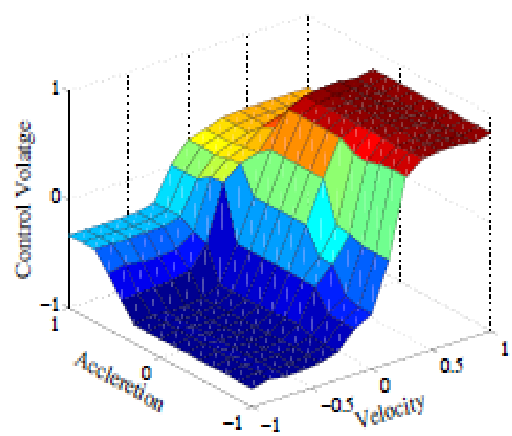

Figure 7: Optimal Fuzzy Rule base

EXPERIMENTAL RESULTS AND NUMERICAL VERIFICATION

Recorded seismic data are used to evaluate the performance of the hybrid control strategy developed in this study. The seismic time-history data are downloaded from the PEER strong motion database [27]. Eight seismic excitations namely Big-Bear, Capemend, Coalinga, Chichi, El-Centro, Loma Prieta, N. Palm Spring and Kobe earthquake records are considered for the experimental study.

Representative figures of the experimental results for a near fault (N. Palm Spring) and far fault seismic motions (El-Centro) are reported. Figs. 8 and 9 show the plot for different test cases under N. Palm Spring and El-Centro earthquake excitations respectively. The experimental and numerical responses are shown together in Fig. 8.

The relative displacements at the base of the isolated structure with simple base isolation and hybrid base isolation are shown in Figs. 8 and 9. Fig. 8 shows an isolator displacement of 0.161 m under near-fault seismic motion, whereas the isolator displacement is only 0.048 m under El-Centro seismic input having far-fault characteristics (see Fig. 9). An analysis of these results brings out the fact that the simple base isolated structures behave differently under different characteristic of seismic motions and is not safe for implementation as a standalone system when active seismic fault is present close to the site of the structure. In such a situation the base isolator needed to be supplemented with a damping device. It is observed that the isolator displacement relative to the ground decreased more for the hybrid control strategy than for the simple base isolated system. In case of N. Palm Spring seismic motion, a peak isolator displacement of 0.161 m with no MR damper condition reduced to 0.005 m (passive-off), 0.001 m (passive-on) control conditions, which are the two extremes of control by MR damper. The variable voltage input to MR damper by SFLC and GAFLC, provides a performance in between the 'passive off' and 'passive on' cases. In the case of SFLC and GAFLC the isolator displacement reduced to 0.0035 m and 0.0028 m, respectively. These numerical values provide two important insights: a) base isolated structures undergo large base displacement under near source, pulse type seismic motion on one hand and b) on the other hand hybrid base isolation with MR damper reduces the large base displacement to within safe limit. Therefore the hybrid base isolation mechanism reduces the drift demand on the isolators in near field earthquakes. This reduction in base displacement comes at a cost of increase in storey responses. The more one restricts the motion at the base (like in passive on case) the more is the super structure responses.

CONCLUSION

This paper provides details of an experimental and numerical study of a three storey hybrid base isolated building. A single MR damper has been used to provide supplemental damping to the isolated structure. Simple FLC and an optimal FLC are employed to monitor the voltage requirement of the MR damper. A geometric strategy has been developed to optimize FLC such that the optimization procedure requires a fewer variables. Micro-GA has been used as an optimization tool. Experimental study has been conducted for fixed base, simple base isolated and hybrid isolation systems. The hybrid isolation consisted of 'passive-off' (0 V), 'passive-on' (2.5 V), manually designed FLC and GA optimized FLC. It has been observed that the simple base isolation system provides efficient vibration control of the structure in far-fault seismic excitations, but undergoes large displacement with an increase in base shear under near-fault seismic excitations. MR dampers along with isolators are effective as an supplemental

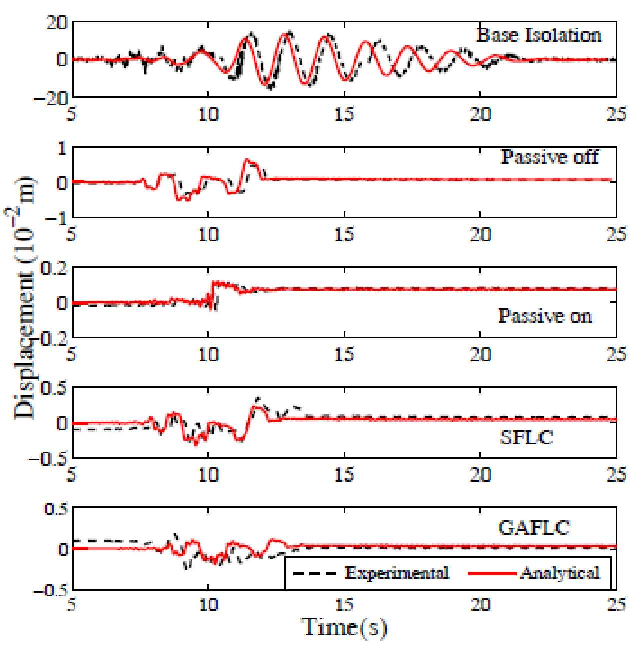

Figure 8 Isolator displacement time histories under N. Palm Spring seismic excitation (experimental and numerical results

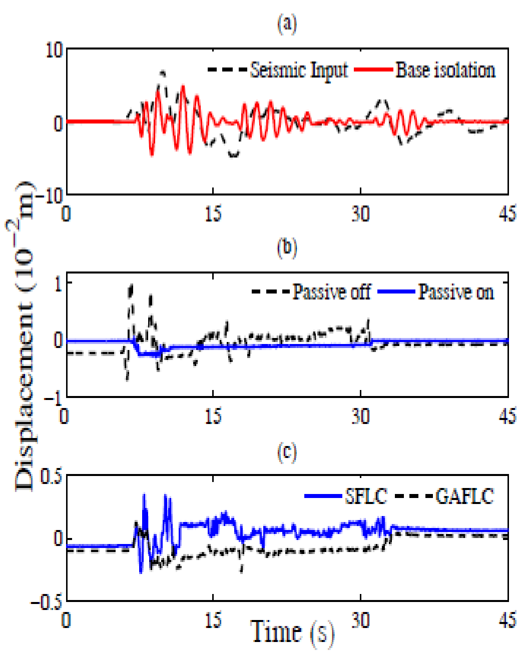

Figure 9. Displacement time history under El-Centro earthquake (experimental results)

damping devices in such situations. MR damper operated in ‘passive-off’ and ‘passive-on’ conditions resulted in totally different control scenarios. In ‘passive-off’ condition base displacements are not reduced efficiently but the base and the structural floor accelerations remain close to their values in the simple isolation case. In contrast, the ‘passive-on’ condition provides a control situation where the displacement at the base is reduced efficiently
at the cost of an increase in base and floor accelerations. Variable damping based on FLC monitored MR damper input voltage has provided a trade-off between the two passive cases and therefore is more suitable for employment with hybrid isolation scheme. Analytical model based simulations and the experimental results are found to have a close comparison. A hybrid system offers a trade-off between a reduction in displacements at the isolation level and an increase in the floor acceleration and inter-story drift levels in the superstructure. The GA-FLC algorithm is able to substantially reduce the isolation level displacements with a marginal increase in the floor acceleration and inter-story drifts in the superstructure, making it an attractive proposition for its implementation.

ACKNOWLEDGEMENT

The authors thank Prof. Anil Agrawal of the Civil Engineering department at City College, CUNY, NY for providing the MR dampers and for the useful discussions we had with him during his visit to IISc.

REFERENCES

[1] T. T. Soong and B. F. Spencer Supplemental energy dissipation: State of the art and state of the practice, Engineering Structures, 24:243–259, 2002.
[2] F. Naeim and J. M. Kelly, Design of Seismic Isolated Structures: From theory to practice, John Wiley & Sons 1999.
[3] J. W. Asher, R. P. Young, and R. D. Ewing Seismic isolation design of the San Bernardino county medical center replacement project, Structural Design of Tall Buildings, 5:265–279, 1996.
[4] N. Makris and S. P. Chang Effect of viscous, visco-plastic and friction damping in the response of seismically isolated structures, Earthquake Engineering & Structural Dynamics, 29:85–107, 2000.
[5] A. K. Agrawal, Z. Xu, and W. L He Ground motion pulse-based active control of a linear base-isolated benchmark building, Structural Control & Health Monitoring, 13(2-3):792–808, 2006.
[6] J. M. Kelly. The role of damping in seismic isolation, Earthquake Engineering & Structural Dynamics, 28:3–20, 1999.
[7] M. D. Symans and S.W. Kelly Fuzzy logic control of bridge structures using intelligent semi-active seismic isolation systems, Earthquake Engineering & Structural Dynamics, 28:37–60, 1999.
[8] A. K. Agrawal, P. Tan, S. Nagarajaiah, and J. Zhang Benchmark structural control problem for a seismically excited highway bridge, part I: Problem definition. http://www-ce.engr.ccny.cuny.edu/People/Agrawal/index.htm, (downloaded: July 2005), 2005.
[9] S Sahasrabudhe and S. Nagarajaiah Experimental study of sliding base-isolated building with magneto-rheological dampers in near fault earthquakes, J. Structural Engineering, ASCE, 131(7):1025–1034, 2005.
[10] S Sahasrabudhe and S. Nagarajaiah Semi-active control of sliding isolated bridges using MR dampers: An experimental and numerical study. Earthquake Engineering & Structural Dynamics, 34(8):965–983, 2005.
[11] G. J. Madden, M. D. Symans, and N. Wongprasert. Experimental verification of seismic response of building frame with adaptive sliding base-isolation system, J. Structural Engineering, ASCE, 128(4):1037–1045, 2002.
[12] J. C. Ramallo, E. A. Johnson, and B. F. Jr Spencer Smart base isolation systems, J. Engineering Mechanics, ASCE, 128(10):1088–1099, 2002.
[13] H. S. Kim, P. N. Roschke, P. Y. Lin, and C. H. Loh. Neuro-fuzzy model of hybrid semi-active base isolation system with FPS bearings and an MR damper, Engineering Structures, 28:947–958, 2006.
[14] D. Shook, P. Y. Lin, T. K. Lin, and P. N. Roschke A comparative study in the semi-active control of isolated structures, Smart Materials & Structures, 16:1433–1446, 2007.
[15] H. Yoshioka, J.C. Ramallo, and B. F. Jr. Spencer ‘Smart’ base isolation strategies employing magneto-rheological dampers. J. Engineering Mechanics, ASCE, 128(5):540–441, 2002.
[16] N. Wongprasert and M. D. Symans Experimental evaluation of adaptive elastomeric base-isolated structure using variable-orifice fluid dampers, J. Structural Engineering, ASCE, 131:867–877, 2005.
[17] H. J. Lee, G. Yang, H. J. Jung, B. F. Jr. Spencer, and I. W. Lee. Semi-active neuro control of a base-isolated benchmark structure, Structural Control & Health Monitoring, 13:682–692, 2005.

[18] Sk. F. Ali and A. Ramaswamy. GA optimized FLC driven semi-active control for phase II smart nonlinear base isolated benchmark building. Structural Control & Health Monitoring, 15(5):797– 820, 2008. DOI:10.1002/stc.272.
[19] D. G. Reigles and M. D. Symans. Supervisory fuzzy control of a base-isolated benchmark building utilizing a neuro-fuzzy model of controllable fluid viscous dampers, Structural Control & Health Monitoring, 13:724–747, 2006.
[20] dSPACE. Release 5, Hardware Card No.-11229, dSPACE GmbH, Germany, URL: http://www.dspace.com, 2005.
[21] MATLAB, The software for Numerical Computing, Version 7.0.1 (R14). The MathWorks, URL: http://www.mathworks.com/index.html?ref=pt, 2004.
[22] Sk. F. Ali and A. Ramaswamy. Testing and modeling of MR damper and its application to SDOF systems using integral back-stepping technique, J. Dynamical Systems, Measurements and Control, 131(2):021009, 2009.
[23] Sk. Faruque Ali Semi-active Control of Earthquake Induced Vibrations in Structures using MR Dampers: Algorithm Development, Experimental Verification and Benchmark Applications, Ph.D Thesis, Indian Institute of Science, Bangalore, India, 2008.
[24] MR Dampers. LORD Technical Data: RD-1005 Damper. http://www.lordfulfillment.com/upload/DS7017.pdf, downloaded: July, 2006, 2006.
[25] B. F. Jr. Spencer, S. J. Dyke, M. K. Sain, and J. D. Carlson, Phenomenological model for magnetorheological dampers. J. Engineering Mechanics, ASCE, 123(3):230–238, 1997.
[26] K., Krishnakumar Micro-genetic algorithms for stationary and non-stationary function optimization, In G. Rodriguez, editor, Proceedings of SPIE Intelligent Control and Adaptive Systems, volume 1196, pages 289–296, November 1989.
[27] PEER. PEER Strong Motion Database. University of California, Berkeley,
URL: http://peer.berkeley.edu/smcat/search.html, 2007.